PHYSICAL REVIEW B VOLUME 55, NUMBER 20 15 MAY 1997-II

Existence of a photonic pseudogap for visible light in synthetic opals

Yu. A. Vlasov, V. N. Astratov, O. Z. Karimov, and A. A. Kaplyanskii
A. F. Ioffe Physical-Technical Institute, Solid State Physics Department, 194021 St.-Petersburg, Russia

V. N. Bogomolov and A. V. Prokofiev
A. F. Ioffe Physical-Technical Institute, Anisotropic Materials Laboratory, 194021 St.-Petersburg, Russia

(Received 16 October 1996)

Synthetic opals, composed of submicron silica spheres close packed in a three-dimensional fcc lattice, are shown to display photonic stop bands at optical frequencies. We have investigated the light attenuation within the stop band as a function of refractive index contrast. Based on measurements of the Bragg attenuation length and on theoretical considerations, we show that a prominent depletion of the photonic density of states (pseudogap) can be achieved in opals by adjusting the volume packing fraction of the spheres and increasing the refractive index of the pores. To approach the pseudogap criterion the pores of opal were impregnated with CdS nanocrystals. We find a dramatic decrease of the attenuation length in opal-CdS, which indicates the strong perturbation of photonic states. [S1063-651X(97)50605-2]

In recent years great interest has been paid to the fabrication and study of artificial three dimensionally (3D) periodic dielectric structures with a period close to the wavelength of electromagnetic (EM) waves.[1] In such photonic crystals the EM waves undergo Bragg diffraction, forming a stop band for modes propagating in a given direction. If the stop bands for all direction of propagation overlap in some frequency range, a photonic band gap (PBG) can be created in which the density of photonic states (DOS) is zero.[2–4] The absence of propagating EM modes inside a PBG can gives rise to unusual quantum optical phenomena such as inhibition of spontaneous emission,[5] Anderson localization of light,[6] etc. The majority of applications of photonic crystals, which utilize their unique optical properties, are expected at optical frequencies. The obtaining of photonic crystals with submicron lattice constants, however, encountered serious difficulties related to the required uniformity and regularity of the photonic lattice on a wavelength scale.[1] Only a few examples of successful fabrication of 3D photonic crystals for the visible spectral region are known to date realized by reactive ion etching[7] and self-ordering of colloids of styrene microparticles.[8]

Recently it was also shown[9–11] that synthetic opals, which are composed of equal diameter a-SiO_2 spheres closely packed in 3D face-centered-cubic (fcc) lattices with periods of about 200 nm, possess photonic stop bands throughout the visible spectrum (400–600 nm). As a result of 3D periodicity of the lattice the stop bands were observed for any direction of incidence[9–11] being mostly pronounced for [111] direction, which was shown to possess the maximal scattering efficiency.[11] The qualitative mapping of opal photonic zones for different critical points (L, K *et al.*) on the surface of the Brillouin zone (BZ) showed that the photonic band structure belongs to a ''semimetallic'' type, characterized by the nonoverlapping stop bands for different directions of propagation.[10,11] This result is in agreement with existing theoretical calculations of photonic band structure in the opal-like fcc photonic lattices composed of spherical ''atoms,''[2,4,12,13] which showed that, due to symmetry restrictions, the complete PBG between the lowest energy zones is absent. It is possible, however, to expel the propagating photonic modes in all but a few directions by adjusting the parameters of photonic lattice: the refractive index contrast between the spheres (n_a) and the surrounding media (n_b) (in the case of opal large n_b can be achieved by filling the pores with various high refractive index materials) and the volume packing fraction of spheres (β) (which can be varied in opals from the fcc close-packed value 0.74 to unity by thermal annealing[11]). Thus, a very large depletion of the photonic DOS, called pseudogap, can be achieved.[12,13] Although the DOS in this case is finite, direct calculations[13] of the emission power of an electric dipole, located in such a type of photonic lattice, have shown that the spontaneous emission should be significantly inhibited in the vicinity of a pseudogap.

In this paper, we present the results of experimental studies and theoretical estimations aimed at an evaluation of the optimal parameters of opal photonic lattices required to achieve the pseudogap. Accurate spectroscopic optical measurements of light attenuation within the stop band in transmission spectra of (111) oriented opal samples reveal an exponential decrease of light intensity with thickness, which arise from Bragg diffraction on a 3D lattice. The Bragg attenuation length L along [111] direction was chosen as a measure of perturbation of photonic modes. We show that the modulation of refractive index contrast in opals, obtained by filling of the pores with various liquids, results in large variations of L. Basing on theory,[2] we provide an estimation of the parameters of the opal photonic lattice (β and n_b) required for the appearance of the pseudogap. We find, that in opal impregnated with CdS nanocrystals, which possesses photonic lattice parameters approaching the criterion of a pseudogap, L exhibits a dramatic decrease down to only 90 lattice constants indicating a strong perturbation of photonic states.

Measurements of the intensity of light beams transmitted through opal samples are complicated by strong diffuse scattering of the incident light from various defects of the lattice,

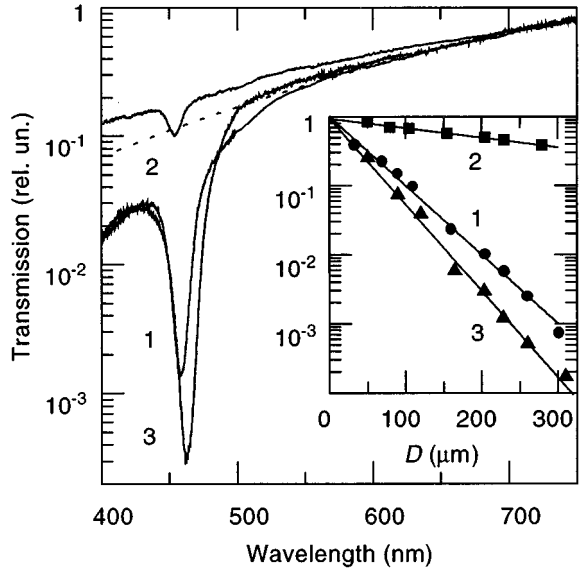

FIG. 1. Transmission spectra of the wedged sample $V18$ taken at incidence normal to the (111) plane for $D=210$ μm. Spectra 1, 2, 3 correspond to different refractive indices of the pores $n_b=1.33$, 1.37, and 1.47. The dotted curve gives the dependence $T\propto\lambda^4$. Inset: Thickness dependences of the attenuation at the center of a stop band. Circles, squares, and triangles correspond to the cases of different n_b. Solid lines are least-square exponential fits to the experimental data.

such as surfaces and bulk defects as vacancies, stacking faults, dislocations, etc.[10,11] In order to minimize the contribution of the diffusely scattered background to the detected signal, the incident beam was highly collimated (divergence less than 1°) and the detection of transmitted light was performed in the direction of incidence within a very narrow angular cone (about 30′). To determine accurately the Bragg attenuation length L, the transmission spectra were measured as a function of the sample thickness D. For this purpose the sample $V18$ (fcc lattice constant $a=276$ nm and $\beta=0.78$, determined by transmission electron microscopy [TEM]) was polished to a form of a wedge of 0.050 rad with a 6 mm long base corresponding to (111) plane. The thickness D was scanned by exact positioning of the wedged sample on a computer-controlled translational stage relative to a fixed 100 μm diaphragm. Figure 1 represents transmission spectra taken from the wedged sample filled with water solutions of α-bromnaphthalene ($1.33<n_b<1.67$) exhibiting a large drop in the vicinity of 460 nm. The reflection spectra measured in the backward direction within the same small angular cone contain a single intense line with the shape and position exactly the same as that of the drop (see also Refs. 9–11). Therefore this drop is defined by diffraction of light on a set of parallel (111) planes and can be referred as a stop band. Normal incidence geometry used in experiments implies that this stop band corresponds to point L on the surface of photonic BZ [11]. It can be seen, that at some intermediate values of $n_b\approx1.37$ (see spectrum 2) the depth of the stop band dramatically decreases, which means that the medium approaches optical homogeneity ($n_a\approx n_b$). The increase of the refractive index contrast results in an increase of the drop for both ''dielectric spheres'' type of lattice ($n_a>n_b$, spectrum 1) and ''air spheres'' type ($n_a<n_b$, spectrum 2). A smooth decline of transmission spectra to shorter wavelengths arises from a partial leakage of light from the detected beam due to scattering. In the long-wavelength region ($\lambda>550$ nm in Fig. 1) it can be approximated by the characteristic Rayleigh powerlike dependence (see dotted curve $T\propto\lambda^4$ in Fig. 1) reflecting an increase of the scattering cross section. The same smooth increase of the intensity of scattered light to shorter wavelengths was also observed in spectra of diffusely scattered light measured within a large angular cone out of the Bragg direction in both forward and backward geometries. Therefore the values of attenuation at the center of the stop band, defined mainly by the Bragg diffraction, can be extracted from the experimental curves in Fig. 1 by subtracting the powerlike dependence through fitting of the long-wavelength tail of each of the spectra. This procedure is valid in assumption that even small angle scattering can contribute to the attenuation observed.

The inset in Fig. 1 depicts thus measured values of attenuation $T(D)$ and reveals an exponential decay of the transmitted light with D. This exponential dependence, which preserves over at least four orders of magnitude (see curve 3), is characteristic for the coherent Bragg diffraction that confirm the validity of the procedure of spectra subtraction. The slope of $T(D)$ gives the values of attenuation length as $L=43$, 310, and 35 μm (or 270, 1900, and 220 lattice planes along the [111] direction) for $n_b=1.33$, 1.37, and 1.47, respectively. The inverse of the attenuation length (imaginary part of the wave vector) reflects the strength of coherent Bragg scattering and, being proportional to the gap width,[14] can be the measure of the overlap of stop bands for different directions. The coherent scattering strength measured for opal-liquid systems appears to be of the same order as for the ordered colloids (the value $L=200$ planes along the [111] direction can be estimated from the results[8]). This value of L is insufficient, however, for a significant depletion of the photonic DOS (for an fcc crystal with $n_a=1$, $n_b=3.5$, and $\beta=0.86$, possessing a pseudogap [5] an attenuation length for microwaves of only a few unit cells was reported).

It has been shown[2] that the scattering strength for a two-component dielectric medium can be estimated from the parameter ϵ_r, which gives the relative fluctuation of the dielectric permittivity from its spatial average

$$\epsilon_r=\left\{\frac{\beta n_a^4+(1-\beta)n_b^4}{[\beta n_a^2+(1-\beta)n_b^2]^2}-1\right\}^{1/2}. \qquad (1)$$

Hence, an increase of ϵ_r should correspond to a decrease of L. Indeed, the ϵ_r values calculated from Eq. (1) for the cases of opal with $n_b=1.33$, $n_b=1.47$, for colloidal systems,[8] and for fcc structure possessing a pseudogap,[5] form the increasing series of $\epsilon_r=0.03$, 0.06, 0.12, and 1.5, respectively. In general, the perturbation parameter ϵ_r plays a crucial role in the photonic band structure. It has been demonstrated[2,3] that, if $\epsilon_r\approx1$ or larger, then significant deviations from the free-photon case, such as a PBG (or a pseudogap, if a PBG is prohibited by symmetry) begin to appear. Figure 2 shows the $\epsilon_r(\beta)$ curves calculated from Eq. (1) for various refractive indices n_a and n_b. When the refractive index contrast is low, ϵ_r reaches a maximum at mean β values around 0.5 for both ''dielectric spheres'' type of lattice (curve 1 corresponds to the case of colloids) and for ''air spheres'' type (curve 4

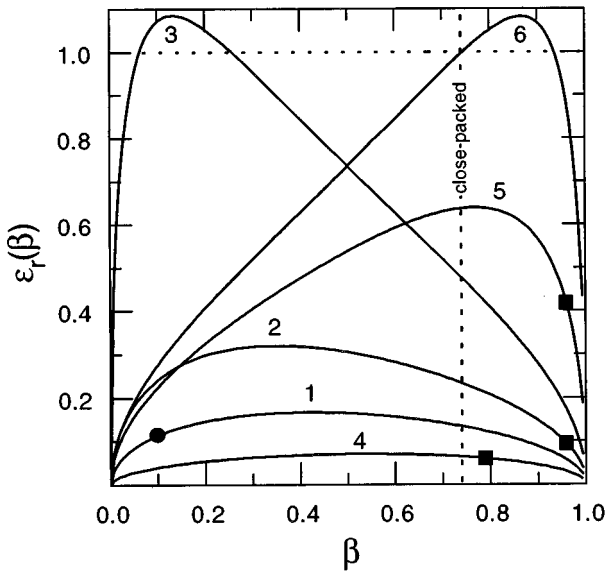

FIG. 2. Plot of $\epsilon_r(\beta)$ calculated from Eq. (1) for ''dielectric spheres'' type of lattices ($n_a=1.57$, 1.37, 2.6 and $n_b=1.33$, 1.0, 1.0 for curves 1, 2, 3, respectively) and for ''air spheres'' type ($n_a=1.37$ and $n_b=1.47$, 2.5, 3.5 for curves 4, 5, 6). Squares correspond to the experimental cases studied. The circle on curve 1 corresponds to estimation of ϵ_r for colloids, according to data of Ref. 8. The horizontal dotted curve represent the criterion for the appearence of a pseudogap $\epsilon_r=1$.

corresponds to the case of opal with $n_b=1.47$). The increase of refractive index contrast results in separation of β regions required for maximizing of ϵ_r: for ''dielectric spheres'' the maximum of ϵ_r is shifted to smaller β (curves 2, 3), while that for ''air spheres'' to the higher β (curves 5, 6). Therefore, taking into account the really attainable β in opal structures ($0.74<\beta<1$), it can be shown that the maximal scattering strength can be achieved in opal photonic lattices of ''air spheres'' type, when the refractive index of the pores n_b is increased by their filling with high refractive index material.

The required parameters can be realized by a complete impregnation of the pores of opal by a semiconductor with an electronic band edge slightly higher in energy than the stop band. For this purpose the opal sample $V21$ ($a=310$ nm, $\beta=0.76$) was impregnated with CdS using vapor phase synthesis.[9–11] The sample was then annealed in a Cd atmosphere to improve the quality of the semiconductor and to obtain values of β higher than close packed. The TEM image of an opal-CdS sample (see Fig. 3) displays the regular package of silica spheres corresponding to a (111) plane. It can be seen that the intrusion of silica spheres into each other appears as a result of annealing, which is accompanied by a decrease of the lattice constant a to 294 nm. The corresponding β value in this sample is increased to about 0.96. A careful analysis of the image reveals small globules of about 5 nm, which form the internal structure of the silica spheres, that can explain the measured values of $n_a\approx1.37$, which are smaller than 1.45–1.5, expected for bulk a-SiO_2. The CdS nanocrystals can be seen as aggregates of dark grains densely concentrated in between the light silica spheres. Selective area diffraction patterns reveal the hexagonal type of CdS nanocrystal lattice of sufficiently good quality.

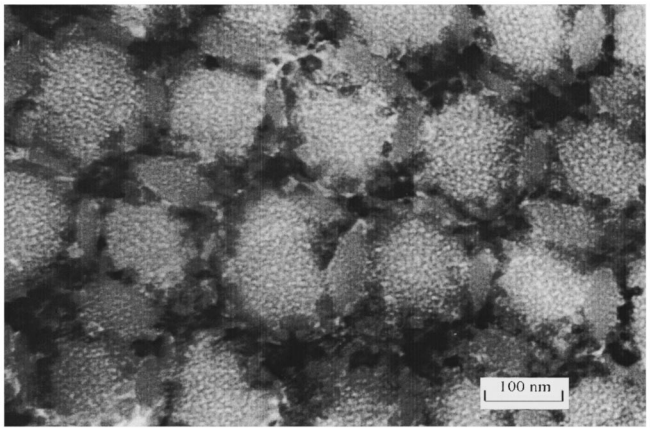

FIG. 3. TEM image of the (111) plane of sample $V21$ impregnated with CdS nanocrystals.

The transmission spectrum of the opal-CdS sample $V21$ ($a=294$ nm, $\beta=0.96$) measured at incidence normal to the (111) plane is presented in Fig. 4 (spectrum 1) in a semilogarithmic scale. The contribution of an incoherent scattering is subtracted according to the procedure described above. The attenuation is plotted in units of cm^{-1} of reciprocal attenuation length $L^{-1}=\ln(I/I_0)/D$, where D is a sample thickness. Besides the clearly seen stop band at 2.1 eV, an additional drastic decrease of transmission appears at energies higher than the A exciton of the bulk CdS (2.47 eV at 300 K, shown by an arrow in Fig. 4), which is due to the absorption of light in the semiconductor. The well-defined oscillations in the transmission spectrum at photon energies of 2.53 eV and 2.63 eV (see second-order derivative curve 3 in Fig. 4) are ascribed to excitonic transitions between the lowest quantum confined electron and hole subbands $H_{0,1}$-$E_{0,1}$ and

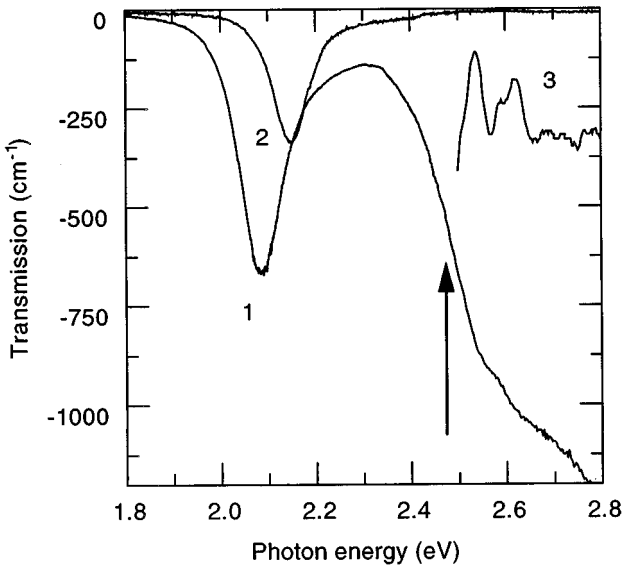

FIG. 4. Transmission spectra of sample $V21$ measured at incidence normal to the (111) plane in the region (1) with embedded CdS nanocrystals and (2) in the reference region. The contribution of incoherent scattering is subtracted as discussed in the text. Curve (3) is a second-order derivative of the spectrum (1). The arrow shows the photon energy of the A exciton of the bulk CdS at 300 K.

$H_{1,1}$- $E_{1,1}$ in nanocrystals of 6 nm diameter. The lower limit of the effective sample volume, occupied by CdS nanocrystals, can be estimated as 1% taking into account the measured absorption of the $H_{0,1}$–$E_{0,1}$ line of about 10^3 cm^{-1} and assuming 10^5 cm^{-1} as typical absorption at an excitonic transition. This value is in agreement with a 4% whole volume of the pores. Therefore at least 25% of the volume of each of the pore is occupied by CdS nanocrystals, which provide a large enough average refractive index n_b.

At energies below the absorption edge of the bulk CdS, the optical stop band can be seen, centered at 2.1 eV. A value of attenuation of about 660 cm^{-1} at the center of a stop band gives an estimation of the attenuation length $L=15$ μm, assuming negligible dissipative losses (the stop band being 400 meV below the absorption edge). The reference transmission spectrum 2 in Fig. 4 was measured from the region of the same *V*21 sample, which was not exposed to a vapor flow during semiconductor synthesis (note the absence of the CdS absorption edge). This region had, however, undergone the same temperature treatments and thus possessed the same β value as the impregnated region. A comparison of the depth of the stop band drops in spectra 2 and 1 shows a dramatic decrease of L from 30 μm to 15 μm, i.e., to about only 90 lattice planes along the [111] direction, indicating the larger perturbation of photonic states caused by enhanced Bragg scattering.

Note, that in the reference region the photonic lattice corresponds to the ''dielectric spheres'' type with $n_a=1.37$ and $n_b=1$ (air in the pores) and Eq. (1) (see curve 2 in Fig. 2) gives $\epsilon_r=0.1$. The redshift of the stop band and the decrease of L observed with filling of the pores with CdS demonstrates that average n_b achieved in opal-CdS become at least larger than n_a. The estimation of the upper limit of ϵ_r for opal-CdS assuming a complete filling of the pore volume with the semiconductor ($n_b=2.5$) gives the value of $\epsilon_r=0.4$ (see curve 5 in Fig. 2). It can be seen from curve 5 in Fig. 2, that even larger values $\epsilon_r=0.64$ (smaller L) can be expected, if we tried $\beta=0.78$ rather than $\beta=0.96$. It can be shown that the point $\epsilon_r=1$ can be reached in opal lattices with $\beta=0.86$ and $n_b=3.3$. Thus in opal impregnated with such semiconductors as ZnTe, GaAs, Ge, Si, etc., a perturbation of photonic states is expected to be large enough for an appearance of a pseudogap. Moreover, a further increase of n_b to 3.5 (see curve 6 in Fig. 2 corresponding to GaAs in the pores) leads to a widening of the appropriate range of β ($0.74<\beta<0.96$), which makes its adjustment during thermal annealing easier.

In conclusion, even though the complete PBG is absent between the lowest-lying bands in fcc lattices with spherical ''atoms,'' the complete PBG between the higher-order bands has been predicted,[2,13] which opens up for $\epsilon_r>1$. Our observations of the second-order stop band in opals[11] allow us to suggest, that in opal filled with a semiconductors with an absorption edge higher in energy than the second-order stop band, the complete PBG can be expected.

We would like to thank Yu. G. Musikhin for providing TEM measurements. This work was supported in part by the Russian Fund for Basic Research, Grant No. 960217928 and by the State Program ''Physics of Solid Nanostructures'' Grant No. 1-061/3.

[1] For a review see articles in *Photonic Band Gaps and Localization*, Vol. 38 of *NATO Advanced Study Institute, Series B: Physics*, edited by C. M. Soukoulis (Plenum, New York 1993); *Photonic Band Gap Materials*, Vol. 315 of *NATO Advanced Study Institute, Series E: Applied Sciences*, edited by E. N. Economou (Plenum, New York, 1996).

[2] H. S. Sözuer *et al.*, Phys. Rev. B **45**, 13 962 (1992).

[3] H. S. Sözuer and J. W. Haus, J. Opt. Soc. Am. B **10**, 296 (1993).

[4] K. M. Ho *et al.*, Phys. Rev. Lett. **65**, 3152 (1990).

[5] E. Yablonovitch, Phys. Rev. Lett. **58**, 2059 (1987); **63**, 1950 (1989).

[6] S. John, Phys. Rev. Lett. **58**, 2059 (1987).

[7] C. Cheng and A. Sherer, J. Vac. Sci. Technol. B **13**, 2696 (1995).

[8] I. Tarhan and G. H. Watson, Phys. Rev. Lett. **76**, 315 (1996).

[9] V. N. Astratov *et al.*, Nuovo Cimento D **17**, 1349 (1995).

[10] V. N. Astratov *et al.*, Superlattices Microstruct. (to be published).

[11] V. N. Astratov *et al.*, Phys. Lett. A **222**, 349 (1996).

[12] Z. Zhang and S. Satpathy, Phys. Rev. Lett. **65**, 2650 (1990).

[13] T. Suzuki and P. K. Yu, J. Opt. Soc. Am. B **12**, 570 (1995).

[14] S. Y. Lin and G. Arjavalingam, Opt. Lett. **18**, 1666 (1993). Note, that the width of the stop band in Fig. 1 also increases with an increase of refractive index contrast. It can be measured, however, with less accuracy than the attenuation length.